NDT and E International 94 (2018) 56–61

Contents lists available at ScienceDirect

NDT and E International

journal homepage: www.elsevier.com/locate/ndteint

Study on in-plane thermal conduction of woven carbon fiber reinforced polymer by infrared thermography

Enqi Wu [a,*], Qian Gao [a], Meihua Li [a], Yufang Shi [a], Andreas Mandelis [b]

[a] School of Mechanical Engineer, University of Shanghai for Science and Technology, Shanghai, 200093, China
[b] Center for Advanced Diffusion-Wave Technologies, University of Toronto, Toronto, Ontario M5S 3G8, Canada

ARTICLE INFO

Keywords:
Woven carbon fiber reinforced polymers
Infrared thermography
Anisotropy
Thermal diffusivity
Porosity

ABSTRACT

Infrared thermography (IRT) is introduced to measure the in-plane thermal conduction of woven carbon fiber reinforced polymers (CFRP). According to the principle of modulated laser heating, the relationship between the phase gradient and the in-plane thermal diffusivity has been deduced, and the experimental platform was established to test the 6 groups of CFRP test specimens with varied porosity. The measured infrared radiation signal was normalized by taking glassy carbon as the reference material, and the Gaussian filtering was applied to removing the noise of infrared thermal images. The experiment results show that the in-plane thermal conduction law in various directions is related to its conduction direction owing to the anisotropy of the CFRP. The in-plane thermal diffusivity of test specimens with different levels of porosity in each direction can be measured when the modulated laser frequency is lower than 1 Hz. In addition, the thermal diffusivity in each direction decreases with the increase of test specimens' porosity.

1. Introduction

With the development of lightweight construction in the aeronautics and astronautics industry, the new materials in the field of composites are developed and optimized. Nowadays safety-critical structures, such as primary aircraft components, are manufactured from carbon fiber reinforced polymer (CFRP) [1], which is a kind of structural material with high strength, light weight, small thermal expansion coefficient, and many other advantages. CFRP is using resin or rubber as matrix and utilizing carbon fiber or its woven fabric as reinforcement. The fiber-woven structure is one of the important factors that affect the thermal physical properties of CFRP, the existence of anisotropy in CFRP also leads to different thermal performance parameters in different directions [2]. It is inevitable that there will be pore during the manufacturing process of CFRP. The existence of pore not only affects the mechanical properties, but also the thermal performance [3]. Therefore, it is significant to study the influence of the pore on the thermophysical parameters of the composites and to analyze the distribution of thermal conduction inside the materials for ensuring the reliability of CFRP. As a consequence, this work deals with the thermal diffusivity of CFRP with varied porosity by using Infrared thermography (IRT).

IRT represents one of the most promising nondestructive testing and evaluation (NDT&E) technique for the inspection of materials and structures through measuring the emitting infrared radiation. It can collect infrared radiation signals from the surface of the object and obtain the thermal diffusivity of the object through signal processing and thermal image analysis [4]. The surface preparation is not required in advance when using IRT to detect the aerospace composite material. The structure parts with complex shape have stronger adaptability using IRT method [5]. This technique has been used in aerospace composite plastic, unglued, fault and other non-destructive testing [6,7]. American scholars began to try to apply this technology in the aerospace field in a variety of equipment in-service real-time monitoring; European countries have carried out the fatigue damage detection of a large force on the building support with sensitive parts, the inspection of the internal defects of steel bar connection parts etc. [8] Therefore, the IRT has great prospects for application in the near future.

In this paper, IRT is used to study the in-plane thermal conduction law of 6 groups of woven CFRP test specimens with different levels of porosity, and the modulation laser scanning frequency is controlled in the range of 0.1–10 Hz. The experimental apparatus and method were introduced in details, and the experimental results show that there is a

* Corresponding author.
E-mail address: weqsd@163.com (E. Wu).

https://doi.org/10.1016/j.ndteint.2017.11.007
Received 28 February 2017; Received in revised form 20 November 2017; Accepted 22 November 2017
Available online 23 November 2017

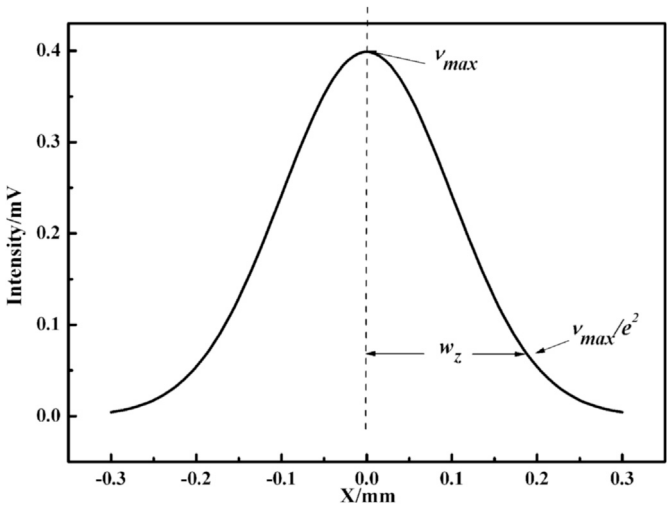

Fig. 1. Gaussian spot lateral distribution.

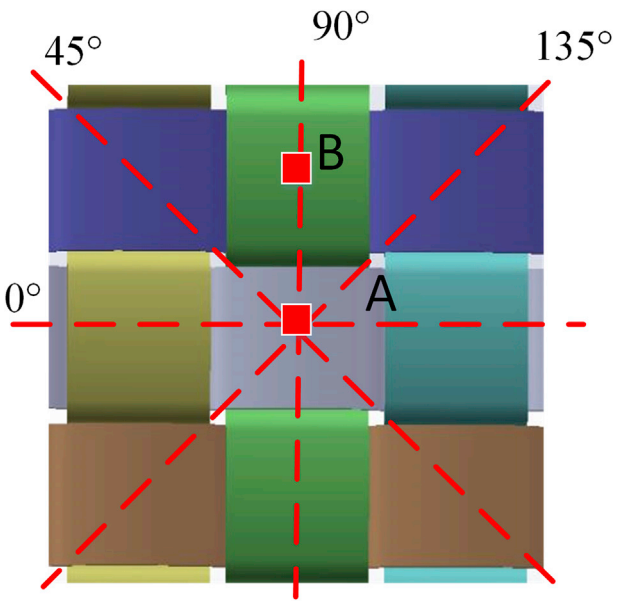

Fig. 2. Structures of fiber preforms.

close relationship between the direction of woven fiber bundle and the in-plane thermal conduction distribution of the CFRP. The thermal diffusivity in each in-plane direction of CFRP can be calculated when the modulation laser scanning frequency is lower than 1 Hz, as a result, the relationship between the thermal diffusivity and the porosity of the CFRP can be obtained.

2. Theory

2.1. Laser-spot periodic heating method

When a modulation laser projected onto the material surface, it will produce a distribution of temperature field on the surface, which is called "thermal wave". A unifying framework for treating diverse diffusion-related periodic phenomena under the global mathematical label of diffusion-wave fields has been developed by Mandelis [9]. In case of a heat source that heats a point on a thin opaque sample with a modulation frequency f, the AC temperature at the point distant r from the heat source is expressed as follows [10]:

$$T_{AC} = T_0 e^{j\left(\omega t - \frac{r}{l} - \frac{\pi}{4}\right)} \frac{-r}{l} r^{-1} \tag{1}$$

Where T_0 is constant, and r is the inverse of the thermal diffusion length l.

Heat wave propagation in the material decays particularly fast, and the propagation distance associates with the modulation frequency f, which can be expressed as follows [11]:

$$k = \sqrt{\pi f/\alpha} = l^{-1} \tag{2}$$

At the point r, the phase θ, with respect to the heat source is expressed as:

$$\theta = -kr - \pi/4 \tag{3}$$

Thermal diffusivity, α, is calculated from the spatial dependence of the phase, $d\theta/dr$, can be expressed as follows:

$$d\theta/dr = -\sqrt{\pi f/\alpha} \tag{4}$$

2.2. Gaussian beam laser

In the ideal state, the infrared radiation phase signal presents Gaussian distribution, its transverse sectional chart was shown in Fig. 1, and the in-plane distribution function can be expressed as follows [12]:

$$\begin{cases} f_T(x) = \dfrac{\nu_{\max}}{2\pi\omega_z^2} \exp\left[-\left(\dfrac{x - x_0}{\sqrt{2}\omega_z} \right)^2 \right] \\ \omega_z = |X_{\nu_{\max}} - X_{\nu_{\max}/e^2}| \end{cases} \tag{5}$$

Where $\nu_{\max}$ is the maximum value of the infrared radiation signal, and ω_z is the equivalent Gaussian width.

The phase value of ω_z can be calculated when knowing $\nu_{\max}$, the phase slope between the phase peak and the equivalent Gaussian width can be obtained by the once degree polynomial fitting. The phase slope is different due to the number of points taken. The R-square correlation coefficient can be obtained in the polynomial fitting. And if the R-square is closer to 1, the phase slope is more reliable. Therefore, $d\theta/dr$ is calculated, and then it is substituted in Equation (4) to obtain α.

3. Experiment

3.1. Test specimen preparation

The CFRP test specimens examined in this study were made of pre-pregs of a plain woven structure and the test specimens were fabricated by using 20 ply laminate, the schematic diagram is shown in Fig. 2. The size of image capture area in the specimen is about 2.5 mm × 2 mm. The direction parallel to the weft yarn is defined as a transverse direction (0°), a direction parallel to the warp yarns is a longitudinal direction (90°), a left diagonal direction to the lower right direction is the main-diagonal direction (45°), the direction along the upper right to lower left is the counter-diagonal direction (135°). Taking the specific structure of woven CFRP into account, point A and point B are projected by the modulation laser during the experiment, and they are located at the intersection of longitudinal and transverse fiber bundles. At point A, the thermal wave propagates transversely in the first layer and longitudinally in the second layer along the fiber bundles. While the thermal wave propagates

Table 1
Porosity and thickness of CFRP test specimens.

No.	S1	S2	S3	S4	S5	S6
Porosity (φ,%)	0.00	0.45	1.55	5.30	10.00	18.32
Thickness (L,mm)	4.25	4.36	4.42	4.66	4.83	5.30

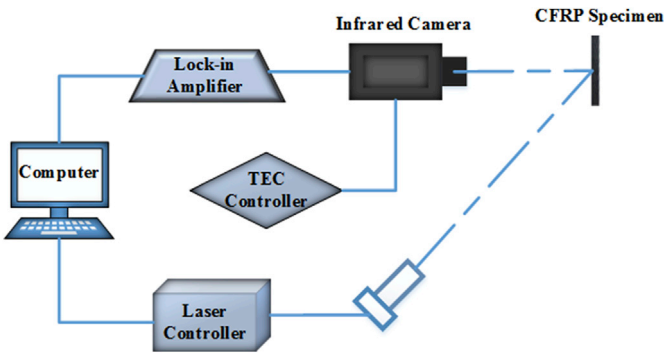

Fig. 3. IRT experiment apparatus.

longitudinally in the first layer and transversely in the second layer at point B.

The content of epoxy resin in prepregs was about 40% by weight, and the plane size of test specimens were all the same (40 mm × 20 mm). The CFRP test specimens with different levels of porosity were prepared by different pressure during the process, and the thickness of the test specimens was varied because of the different porosity. The properties of CFRP test specimens are shown in Table 1. It can be seen from Table 1 that the thickness of the test specimens increases with the increase of porosity.

3.2. Apparatus and measurements

The schematic diagram of experimental apparatus for the CFRP thermal performance testing is shown in Fig. 3. This system mainly consists of infrared camera (FLIR-SYSTEMS-INC SC7000), laser diode (JENOPTIK, 808 nm), laser controller (Thorlabs, LDC210C), lock-in amplifier (SR850), TEC controller, data acquisition and processing system. The laser is modulated by the driver and directly projected onto the surface of the test specimen, which is placed vertically, and then the infrared radiation phase signal generated by the test specimen is received by the infrared camera. The Lock - in amplifier is directly connected with the computer. The collected signal is recorded and processed by the computer.

In order to improve the sensitivity and SNR (Signal to Noise Ratio) of the acquired signal, the intensity of light source should be increased appropriately. The modulation laser scanning frequency range is 0.1–10 Hz, and the laser generates beam whose maximum output power is 20 mW. The form of the incident laser beam is Gaussian and its diameter is about 0.2 mm. In order to eliminate the influence on the signal acquisition from the experimental equipment system, the same experiment was carried out with glassy carbon as the reference material for normalization, then using Gaussian filter to remove noise from the obtained image signal.

4. Experimental results and analysis

The Infrared radiation phase images of S1 at point A are shown in Fig. 4 when the laser modulation frequency is 0.1 Hz. It can be seen from the figure that the infrared radiation phase image is composed of 128 × 160 pixels, the maximum infrared radiation phase value is located at the laser heating point, and the phase value is gradually reduced with the increase of distance away from the laser heating point.

4.1. Relationship between phase value and frequency

The relationship between the maximum phase value and the modulation frequency for the six test specimens at point A is shown in Fig. 5

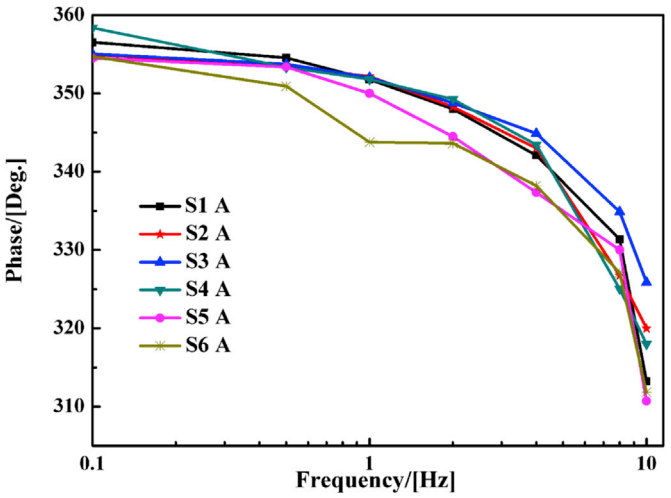

Fig. 5. Phase versus frequency.

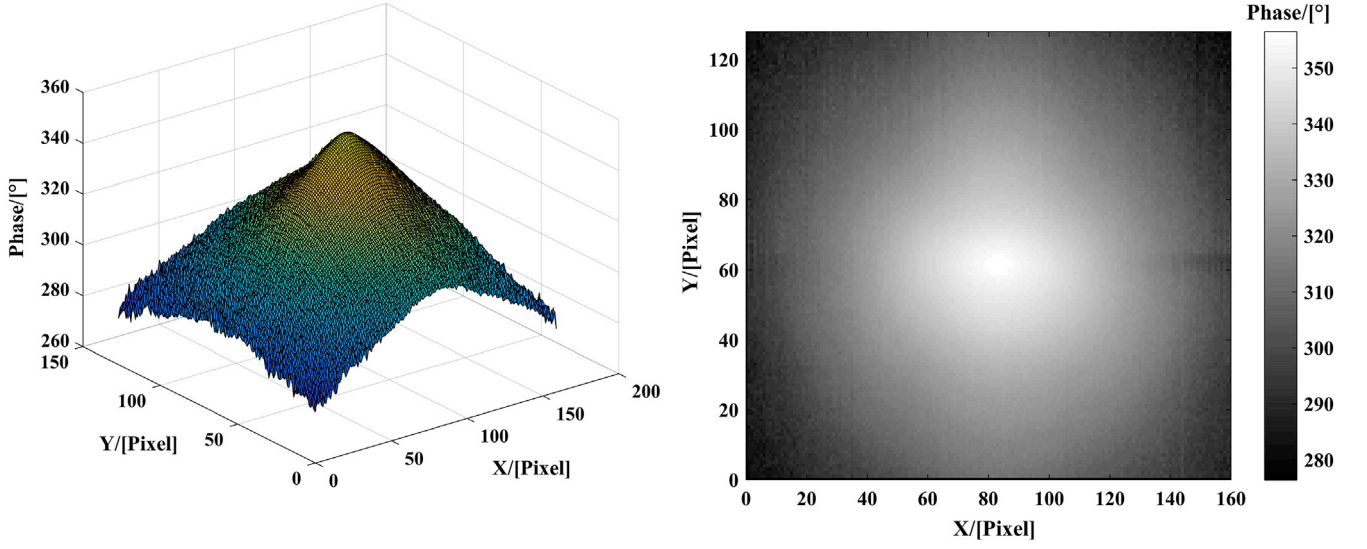

Fig. 4. Infrared radiation phase image.

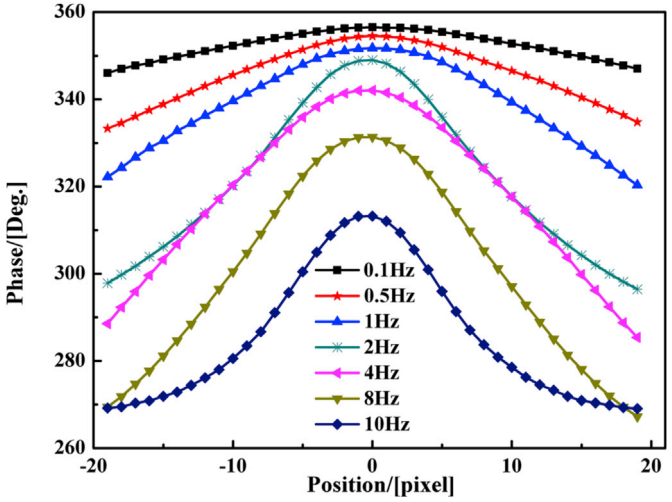

Fig. 6. Phase distribution under different modulated frequency.

when the laser modulation frequency is 0.1–10 Hz. According to eq. (1), the phase shift must be negative, and they close to zero. We added by 2π to simplify the calculation without affecting the analysis result. It can be seen from the figure that the phase of the test specimens are different due to the unique woven structure of CFRP, but the overall variation trend is consistent. The higher the frequency, the phase lag become more obvious.

4.2. Relationship between phase signal distribution and frequency

Taking transverse thermal conduction of S1 at point A for analysis, the distribution of the infrared radiation phase signal in different laser modulation frequency is shown in Fig. 6. It can be seen from the figure that the phase slope and the equivalent Gaussian width are different at different laser modulation frequency; the phase slope at high frequency is significantly larger than that at low frequency, and the equivalent Gaussian width at low frequency is obviously larger than that at high frequency.

4.3. Analysis for anisotropic distribution

Fig. 7 shows the phase contour map of S1 at point A under different modulation frequency. As shown in the figure, the thermal radiation area decreases with the increase of the modulation frequency, and presents the concentric ellipse shape distribution. In the 6 groups of CFRP test specimens, the material of warp yarn and weft yarn is the same, and the heat wave propagates along the direction of the fiber bundle, the distribution of the resin and the pores in each direction is different, which leads to different thermal diffusion level in each direction. It proved that CFRP is an anisotropic material, the thermal diffusion length (l) decreases with the increase of the modulation frequency (f). Therefore, the centrifugal rate of elliptical contour decreases with the increase of the modulation frequency, the phase contour map gradually forms a concentric circle.

Fig. 8 shows the infrared radiation phase signal distribution of S1 at point A in four directions when the laser modulation frequency is 0.5 Hz. It can be seen from the figure that the thermal conduction distribution in the transverse, longitudinal, main-diagonal and counter-diagonal direction is different. It is proved that the internal inhomogeneity of CFRP material is caused by the lamination, and it exactly indicates that CFPR has the characteristics of anisotropy. The phase slope in the transverse (0°) and longitudinal (90°) directions varies significantly to each other, and the phase slope in the main-diagonal (45°) and the counter-diagonal (135°) directions is close to each other.

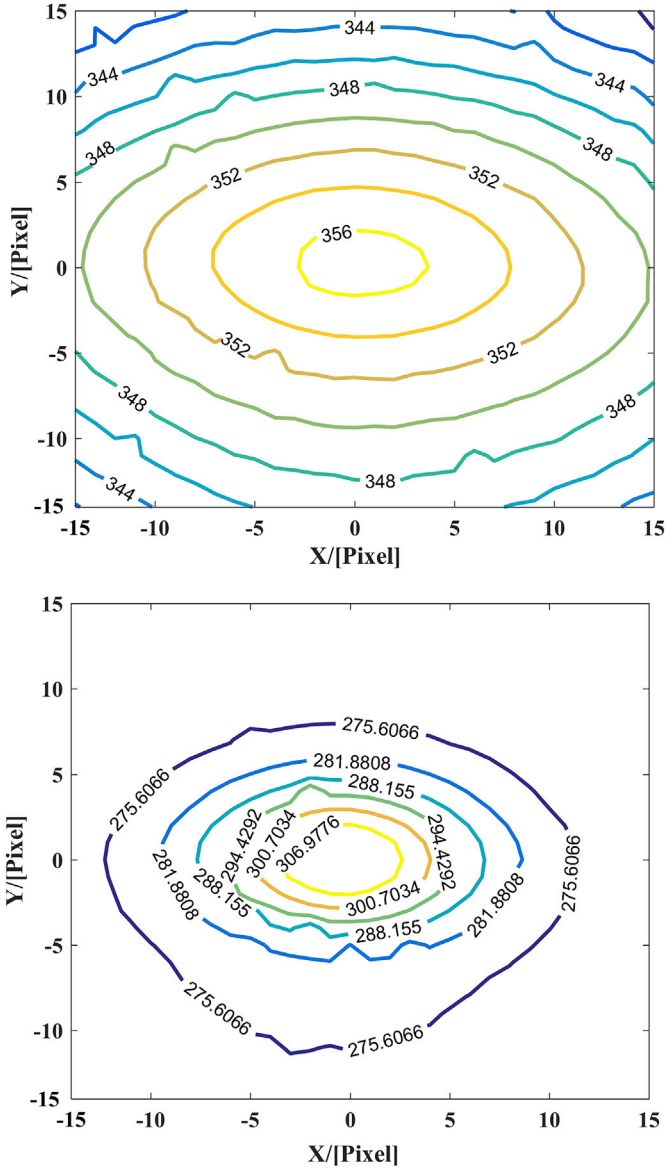

Fig. 7. Phase contour maps under different frequency.

4.4. Calculation of thermal diffusivity

According to reference [1], the thermal diffusivity of CFRP in the thickness direction can be obtained. The thermal diffusion length ($\mu_{1Hz}, \mu_{2Hz}, \mu_{4Hz}$) in the thickness direction of six test specimens at the laser modulation frequency of 1 Hz, 2 Hz, 4 Hz can be calculated by equation (2), then comparing it with the thickness of the single-layer prepreg laminate (T_{SL}) of the six test specimens, the results are shown in Fig. 9. As can be seen from the figure, the thermal diffusion length of the six test specimens (μ_{1Hz}) are larger than the thickness of single-layer prepreg laminate (T_{SL}) when the laser modulation frequency is 1 Hz, it means the laser can at least penetrate a single-layer prepreg laminate. At this point, the infrared radiation signals can fully reflect the thermal conductivity of CFRP. Moreover, the thermal diffusion length is gradually reduced with the increase of the laser modulation frequency, the thermal performance of the CFRP cannot be correctly reflected by the infrared radiation signal under this circumstance. Therefore, taking the average value of the thermal diffusivity calculated from 0.1 Hz、0.5 Hz and 1 Hz as the thermal diffusivity of the CFRP test specimens.

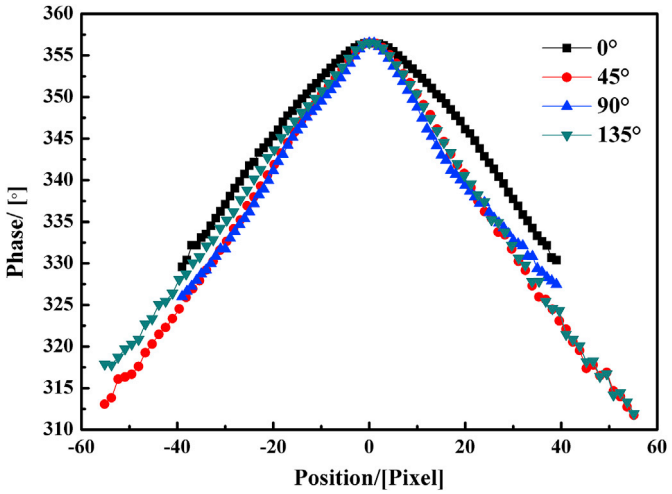

Fig. 8. Phase distribution on four directions.

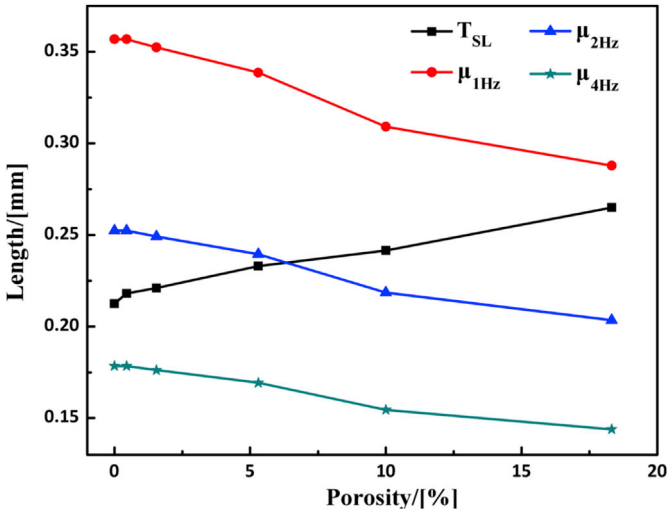

Fig. 9. Thermal diffusion length versus thickness of single-layer prepreg laminate.

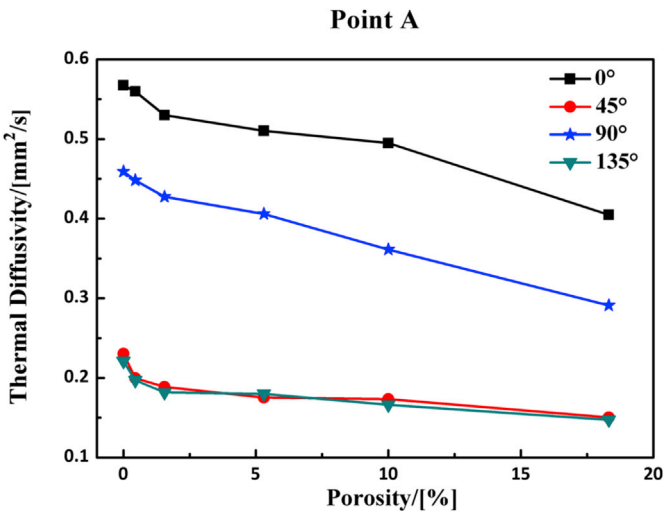

Fig. 10. Thermal diffusivity versus porosity at point A.

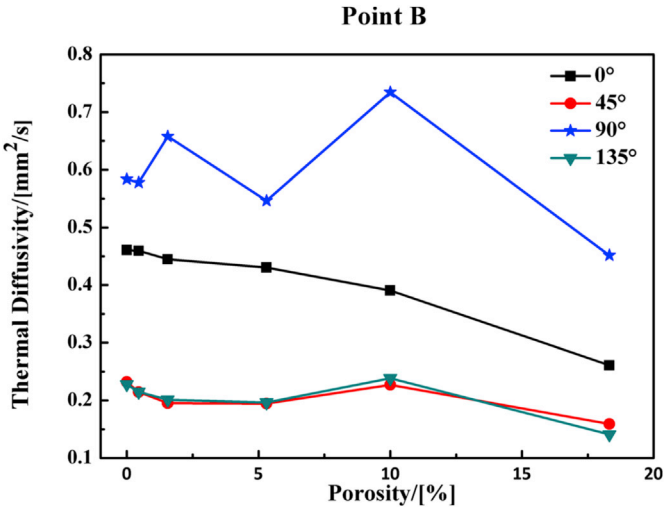

Fig. 11. Thermal diffusivity versus porosity at point B.

4.5. Relationship between thermal diffusivity and porosity

By analyzing the thermal diffusivity of six test specimens in four directions calculated from point A and point B, the relationship between thermal diffusivity and porosity is shown in Figs. 10 and 11.

It can be seen from Fig. 10 that at point A, the thermal diffusivities of the test specimens in the woven plane of the fiber bundle are not the same in all directions The thermal diffusivity at the woven direction of upper prepreg laminate (0°) is in the maximum, followed by the woven direction of bottom prepreg laminate (90°), and the minimum thermal diffusivity is at the main-diagonal direction (45°) and counter-diagonal direction (135°). Besides, the thermal diffusivity in the four directions decreases with the increase porosity of test specimens.

As can be seen from Fig. 11, at point B, the thermal diffusivity of test specimen S3 and S5 in the longitudinal direction increases sharply. But in fact, the thermal diffusivity won't change suddenly when the experimental temperature is unchanged, and the thermal diffusivity is only related to the thermal conductivity, density and specific heat capacity of the CFRP material. Therefore, it may be uncertainty of the resin and porosity in the heat conduction direction that caused the thermal diffusivity mutation.

Table 2
Thermal diffusivity on 0° and 90°.

Position	Direction	α[mm²/s]			
		S1	S2	S4	S6
Point A	0°	0.568	0.560	0.510	0.405
	90°	0.459	0.448	0.406	0.291
Point B	0°	0.461	0.459	0.430	0.261
	90°	0.584	0.578	0.546	0.452

Since the thermal wave diffuses along the direction of fiber bundle, and the thermal diffusivity value (α) on 0° and 90° directions at point A and point B in four test specimens (S1,S2,S4,S6) is shown in Table 2. It can be seen from the table that the thermal diffusivity value on 0° and 90°directions at point A is similar to that in the 90° and 0° directions at point B respectively, which is because the laser is directly projected on the transverse fiber bundle at point A, while it is projected on the longitudinal fiber bundle at point B. Therefore, the carbon fiber woven structures directly affect the in-plane thermal conduction of CFRP.

5. Conclusion

According to the principle of modulated laser heating, infrared thermography is used for analyzing the in-plane thermal conduction of woven carbon fiber reinforced polymer. The experiment results show that the unique woven structure of CFRP makes it anisotropic, and the thermal conduction law of CFRP in the plane direction of the fiber bundle is related to its conduction direction. The shape distribution of the infrared radiation phase contour map presents a concentric ellipse, and the centrifugal rate increases with the decrease of the modulation frequency. When the modulated frequency is lower than 1 Hz, the in-plane thermal diffusivity of test specimens in each direction can be measured, and the thermal diffusivity decreases with the increase of porosity. Therefore, the woven structure, resin distribution and porosity content have a direct effect on the thermal diffusivity. It is found that the measurement results were affected by the measurement location due to uneven pore distribution of the test specimens. And some results even do not meet influence law of porosity on thermal diffusivity. Further studies about the measurement errors and uncertainties caused by the uneven pore distribution and the shape of the pores will be conducted in the future research.

Funding

National Natural Science Foundation of China [grant number: 51205255]; The National Key Technology R&D Program [grant number: 2015BAK16B04].

References

[1] Mayr G, Plank B, Sekelja J, et al. Active thermography as a quantitative method for non-destructive evaluation of porous carbon fiber reinforced polymers. NDT&E Int 2011;44:537–43.
[2] Kaiyuan Li, Yongdong Xu, Litong Zhang, et al. Effects of fabric architectures on the thermal expansion coefficient and the thermal diffusivity of carbon fiber reinforced silicon carbide composites. J Chin Ceram Soc 2008;36(11):1564–9.
[3] Meola Carosena, Toscano Cinzia. Flash thermography to evaluate porosity in carbon fiber reinforced polymer (CFRPs). Materials 2014;7:1483–501.
[4] Sfarra S, Regi M, Santulli C, et al. An innovative nondestructive perspective for the prediction of the effect of environmental aging on impacted composite materials. Int J Eng Sci 2015;102:55–76.
[5] Theodorakeas P, Avdelidis NP, Hrissagis K, et al. Automated transient thermography for the inspection of CFRP structures: experimental results and developed procedures. SPIE 2011;8013:80130W.
[6] Dapeng Chen, Zhi Zeng, Cunlin Zhang, et al. Air-Coupled ultrasonic infrared thermography for inspecting impact damages in CFRP composite. Chin Opt 2012; 10(s1):s10401.
[7] Sfarra S, Perilli S, Paoletti D, et al. Ceramics and defects. Infrared thermography and numerical simulations e a wide ranging view for quantitative analysis. J Therm Anal Calorim 2016;123:43–62.
[8] Zhi Zeng, Jing Zhou, Ning Tao, et al. Absolute peak slope time based thickness measurement using pulsed thermography. Infrared Phys Technol 2012;55(2–3): 200–4.
[9] Mandelis A. Diffusion-wave fields: mathematical methods and green functions. New York: Springer; 2001.
[10] Enqi Wu, Zihong Xu, Xinxin Guo, et al. Influence of porosity on photothermal radiometry of carbon fiber reinforced polymers. Chin J Lasers 2015;42(7), 0706006.
[11] Kuribara Masaya, Nagano Hosei. Anisotropic thermal diffusivity measurements in high-thermal- conductive carbon-fiber-reinforced plastic composites. J Electron Cool Therm Control 2015;5:15–25.
[12] Yuqing Chen, Jinghuan Wang. Laser principle. Hangzhou: Zhejiang University Press; 1992.